

Supplementary information

Cationic porphycenes as potential photosensitizers for antimicrobial photodynamic therapy

Xavier Ragàs,^{†,‡} David Sánchez-García,[†] Rubén Ruiz-González,[†] Tianhong Dai,^{‡,⊥}
Montserrat Agut,[†] Michael R. Hamblin,^{‡,⊥,#} and Santi Nonell^{*,†}

[†]*Institut Químic de Sarrià, Universitat Ramon Llull, Barcelona 08017, Spain; [‡]Wellman Center for Photomedicine, Massachusetts General Hospital, Boston, Massachusetts 02114, USA;*

[⊥]*Department of Dermatology, Harvard Medical School, Boston, Massachusetts 02115, USA;*

[#]*Harvard-MIT Division of Health Sciences and Technology, Cambridge, Massachusetts 02139, USA*

Part I. NMR Spectra

Part II. HPLC Analysis of Py₃MeO-TBPO

Part III. Fluorescence quantum yields

Part IV. Singlet oxygen quantum yields

Part V. *In vitro* photoinactivation of bacteria

Part VI. *In vitro* photoinactivation of fungi

Part I. NMR spectra

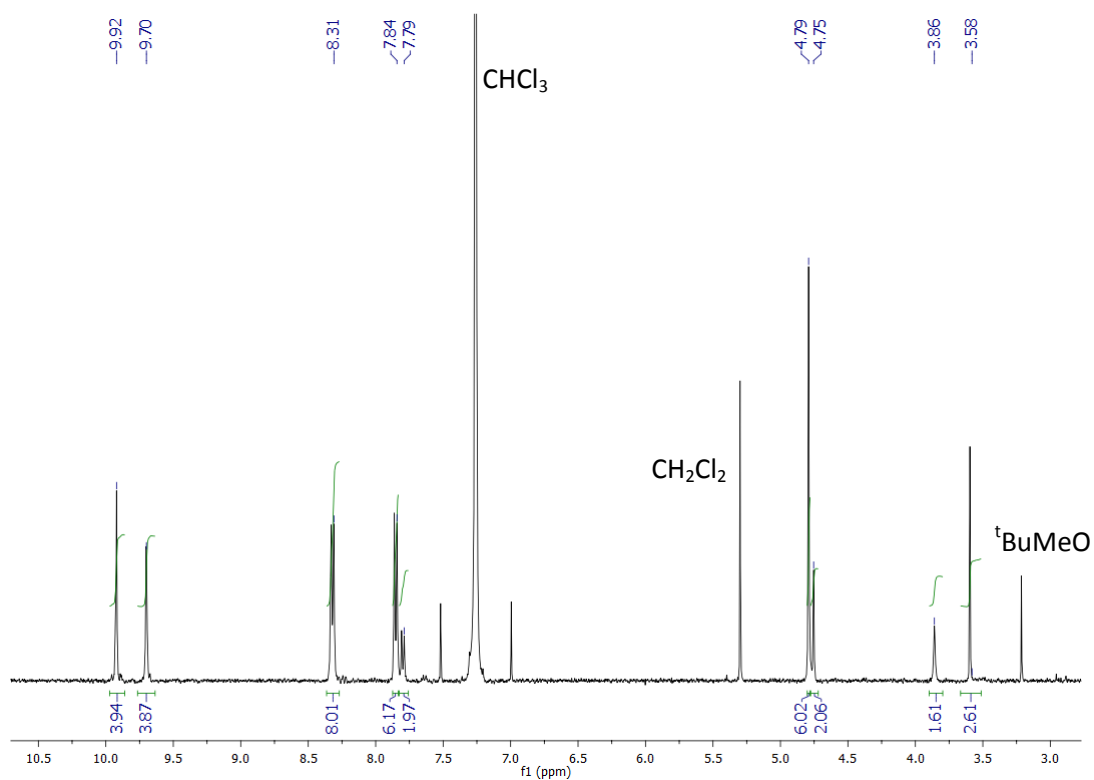


Fig. S1. $^1\text{H-NMR}$ spectrum of $\text{Br}_3\text{MeO-TBPo}$ in CDCl_3 .

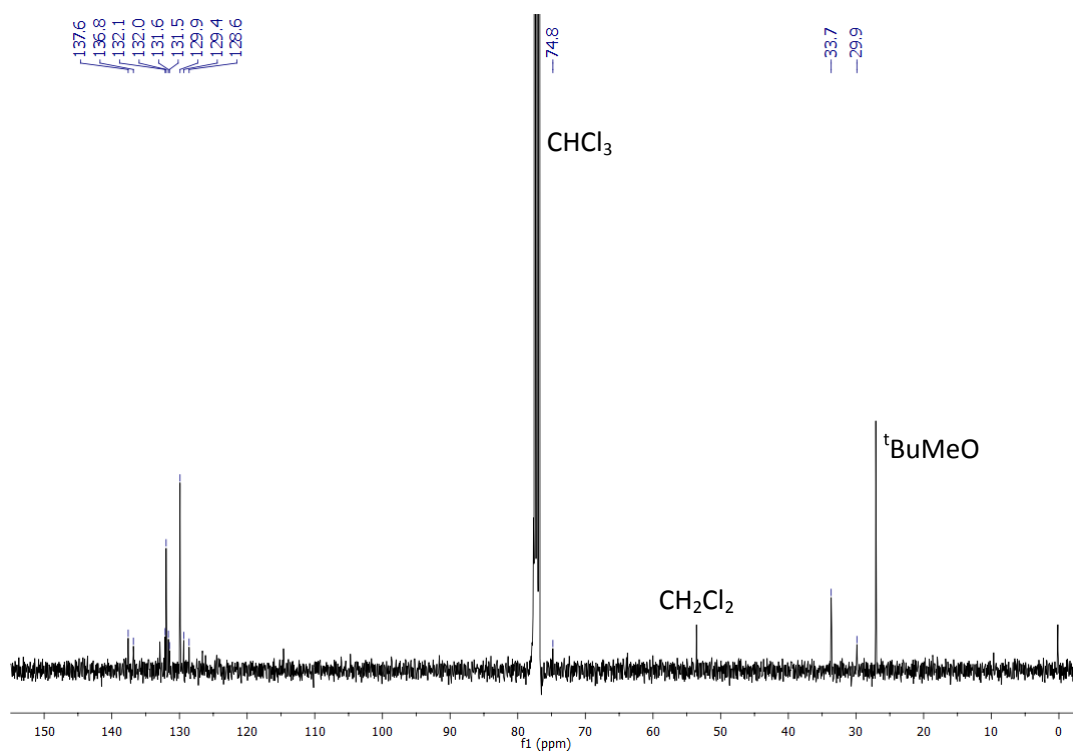


Fig. S2. $^{13}\text{C-NMR}$ spectrum of $\text{Br}_3\text{MeO-TBPo}$ in CDCl_3 .

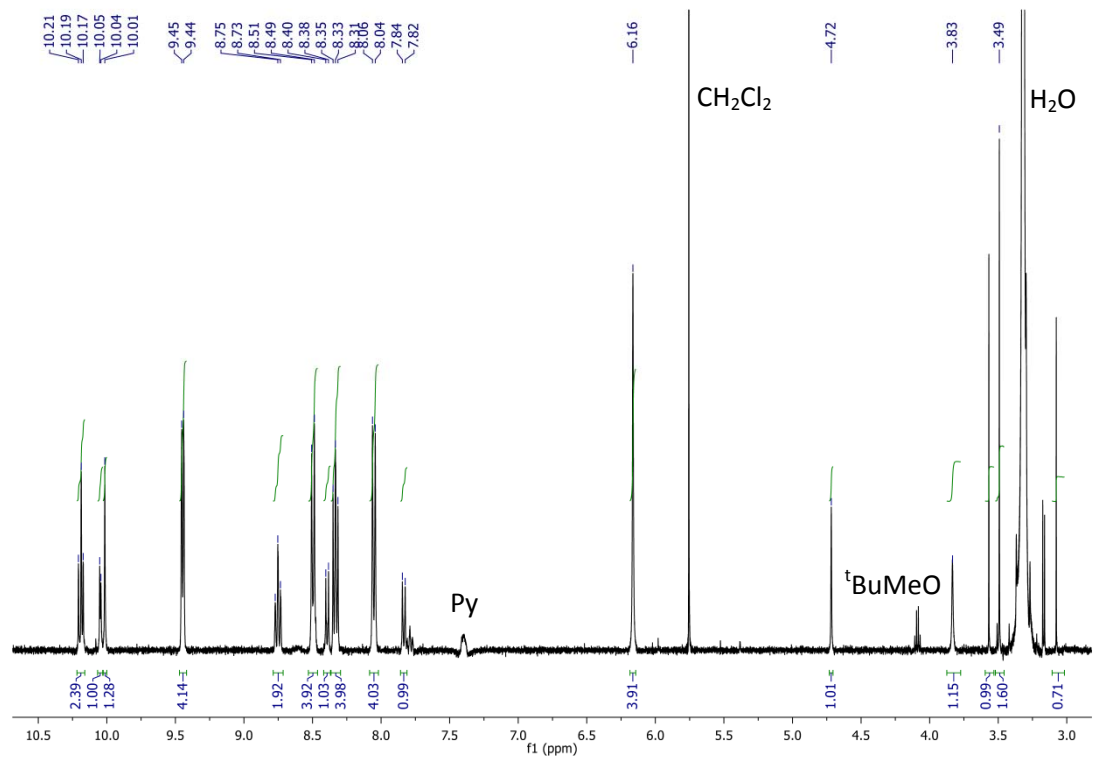


Fig. S3. $^1\text{H-NMR}$ spectrum of $\text{Py}_3\text{MeO-TBPO}$ in $\text{d}_6\text{-DMSO}$.

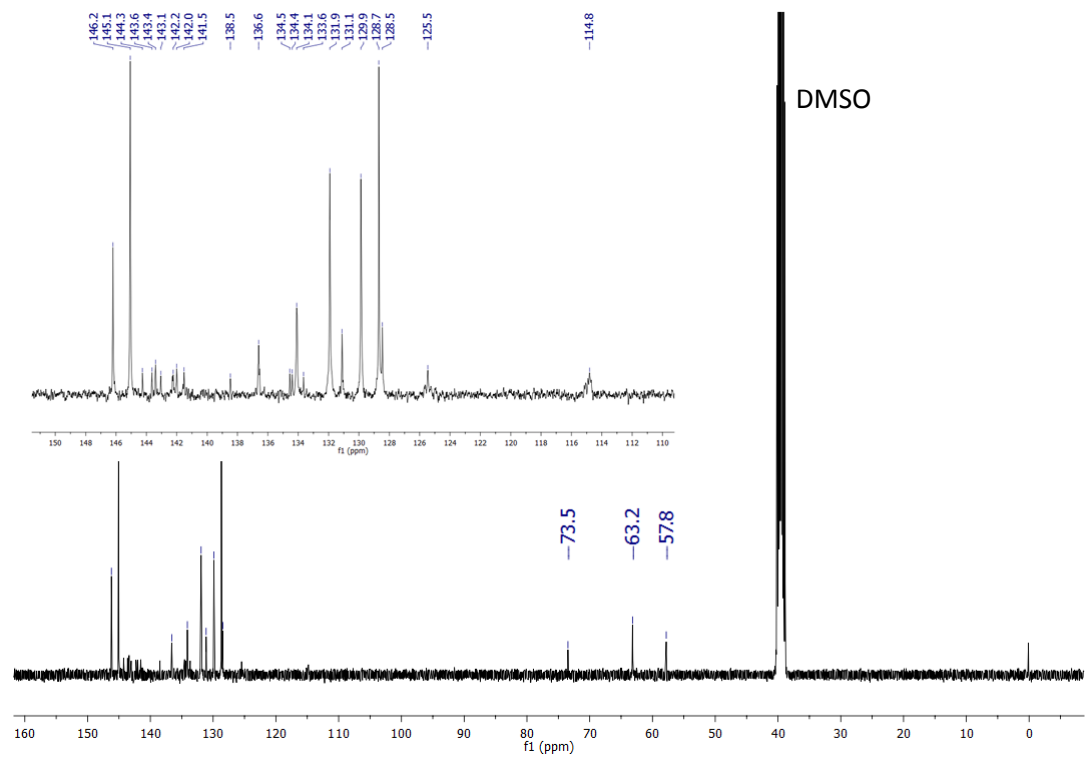


Fig. S4. $^{13}\text{C-NMR}$ spectrum of $\text{Py}_3\text{MeO-TBPO}$ in $\text{d}_6\text{-DMSO}$. Inset: Zoom from 110 to 150 ppm.

Part II. HPLC analysis of Py₃MeO-TBPO

Liquid Chromatography (HPLC) was performed with an Agilent 1200 series liquid chromatograph equipped with a diode array detector. Py₃MeO-TBPO was analyzed on a 30 mm x 4 mm, 3 μ m particle, Lichrocart Purospher STAR RP-18E column. Detection was achieved at three wavelengths, 244, 380 and 650 nm. All chromatography runs were performed at 50 °C with a mobile phase flow rate of 2.0 mL min⁻¹. Isocratic elution was performed with 50:50 ACN/aqueous solution, which contained 25 mM sodium dodecyl sulfate and KH₂PO₄ 0.01M, adjusted to pH = 4.

As shown in Figure S5, a single peak can be observed at 8.6 min, irrespective of the detection wavelength.

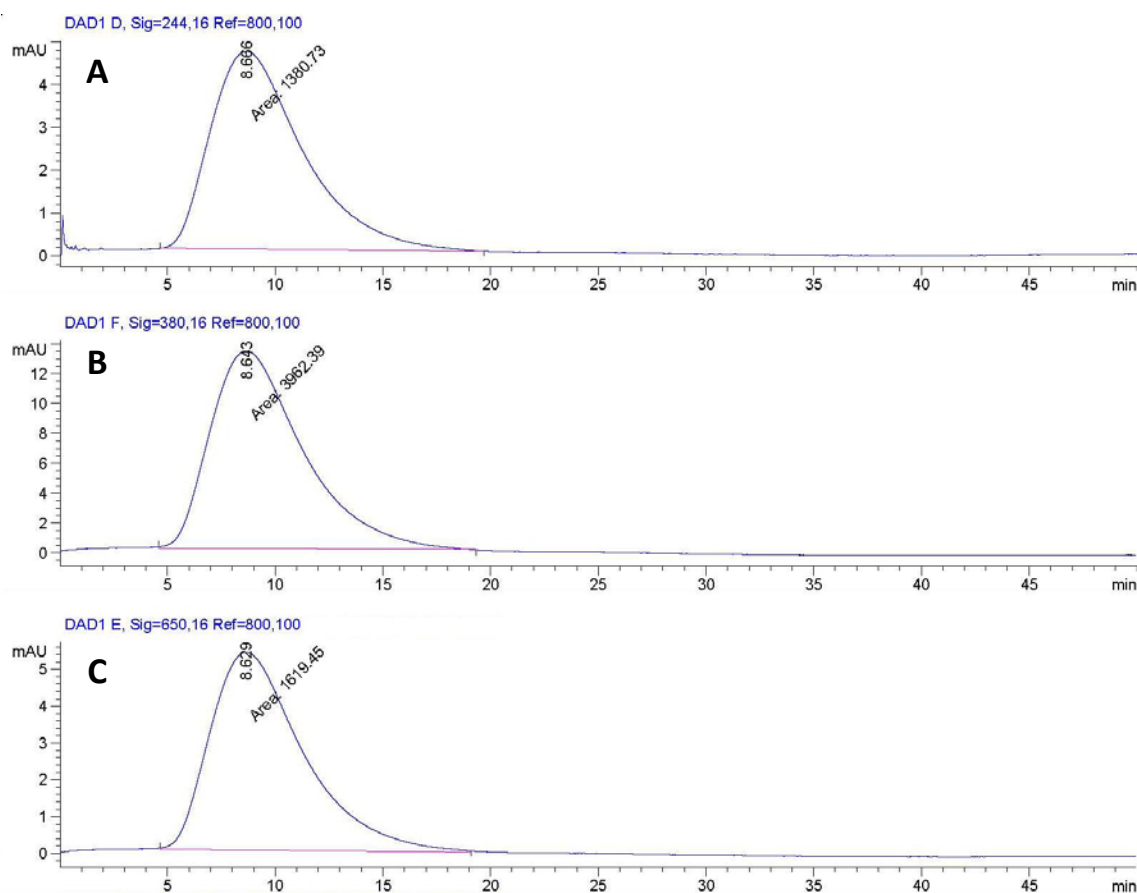


Figure S5. Liquid chromatography of Py₃MeO-TBPO detected at (A) 244 nm, (B) 380 nm and (C) 650 nm.

UV-Vis spectra were recorded every 1 s and found to be identical throughout the peak (Figure S6).

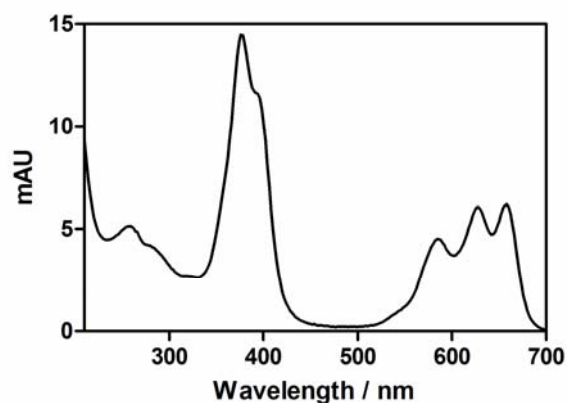


Figure S6. Absorption spectrum of the Py₃MeO-TBPO peak at 8.6 min obtained by liquid chromatography and diode array detection.

Part III. Fluorescence quantum yields

The fluorescence quantum yield, Φ_F , was determined by means of equation 1:

$$\Phi_F(\text{sample}) = \frac{\overline{F}_{\text{sample}} \cdot n_{\text{sample}}^2}{\overline{F}_{\text{ref}} \cdot n_{\text{ref}}^2} \cdot \Phi_F(\text{ref}) \quad \text{Equation 1}$$

where F_i is the fluorescence intensity integrated over the entire emission spectrum corrected by the absorption factor ($1 \cdot 10^{-A}$) and n_i is the refractive index of the solvent used in each case.

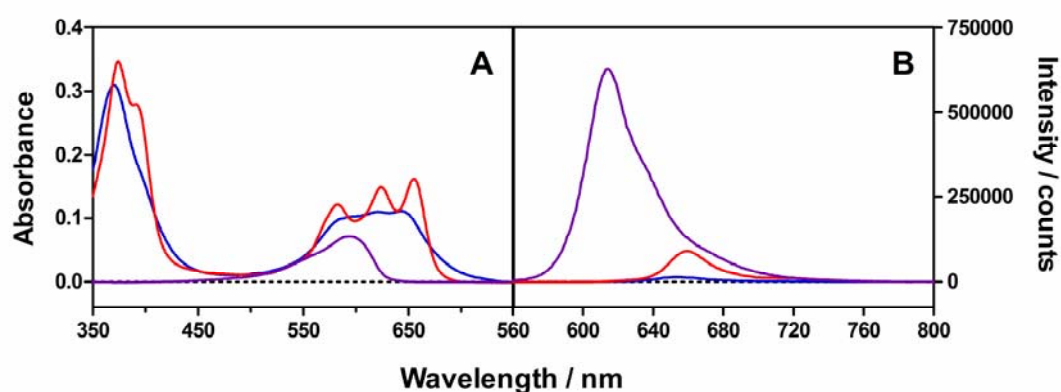


Fig. S7. (A) Absorption and (B) fluorescence spectra of cresyl violet in MeOH (violet), and Py₃MeO-TBPO in water (blue) and in MeOH (red).

The absorption and emission spectra of optically-matched solutions at 532 nm of cresyl violet in MeOH as reference, and porphycene solutions in MeOH and aqueous media is shown in Figure S1.

Part IV. Singlet oxygen quantum yields

The quantum yield of singlet oxygen photosensitisation is defined as the number of photosensitized $^1\text{O}_2$ molecules per absorbed photon. The pre-exponential factor $S(0)$, which is proportional to Φ_Δ , was determined by fitting equation 2 to the time-resolved phosphorescence intensity at 1270 nm.

$$S(t) = S(0) \cdot \frac{\tau_\Delta}{\tau_T - \tau_\Delta} \cdot \left(e^{-t/\tau_T} - e^{-t/\tau_\Delta} \right) \quad \text{Equation 2}$$

The quantum yields of $^1\text{O}_2$ production were determined by comparison of $S(0)$ to that produced by an optically matched reference in the same solvent and at the same excitation wavelength and intensity (Equation 3).

$$\Phi_\Delta (\text{sample}) = \frac{S(0)_{\text{sample}}}{S(0)_{\text{ref}}} \cdot \Phi_\Delta (\text{ref}) \quad \text{Equation 3}$$

Part V. *In vitro* photodynamic inactivation of bacteria

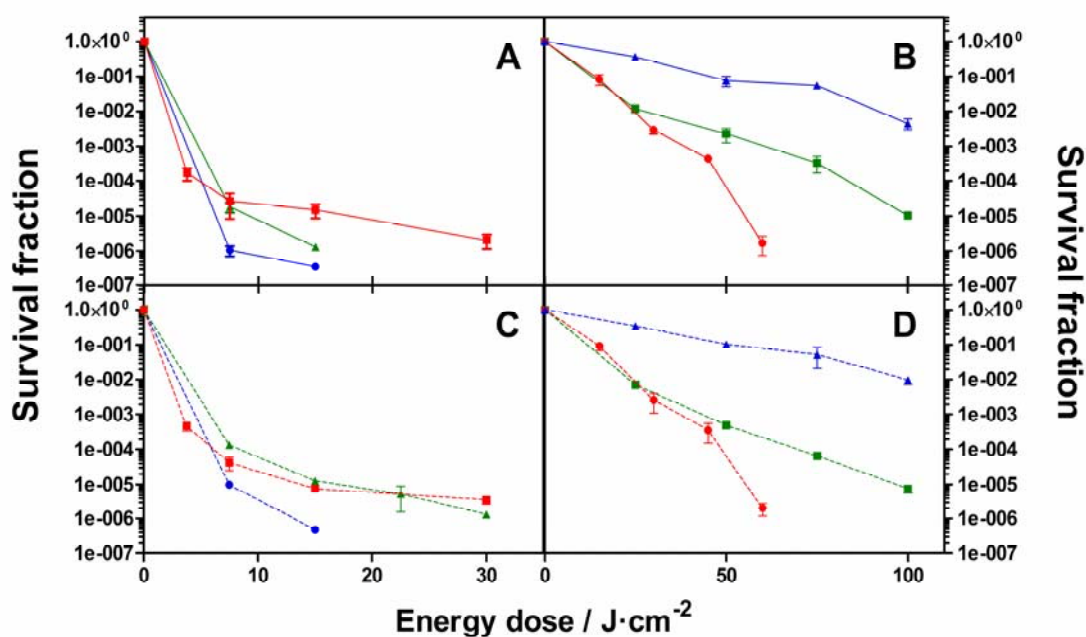


Figure S8. Light-dose response inactivation curves of bacteria upon irradiation with light of 652-nm at 125 mW·cm⁻². (A, C) Survival curves of MRSA (triangles), *S. aureus* (circles), *E. faecalis* (squares) with (dashed line) and without (solid line) removing the excess of PS from the solution with a bulk concentration of Py₃MeO-TBPO of 0.5 μM (*E. faecalis*) and 1 μM (MRSA and *S. aureus*). (B, D) Survival curves of *A. baumannii* (squares), *E. coli* (circles), *P. mirabilis* (triangles) with (dashed line) and without (solid line) removing the excess of PS from the solution with a bulk concentration of 5 μM (*A. baumannii* and *E. coli*) and 20 μM (*P. mirabilis*). Error bars show the standard error of the mean of 3 different experiments.

Part VI. *In vitro* photodynamic inactivation of fungi

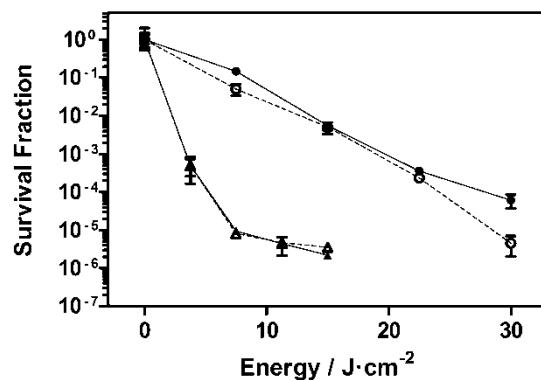


Figure S9. Light-dose response inactivation curves of *C. albicans* (circles) with light of 652-nm and *C. krusei* (triangles) with light of 635-nm. Survival curves with (dashed line) and without (solid line) removing the excess of PS from the solution with a bulk concentration of Py₃MeO-TBPO of 20 μ M for *C. albicans* and 10 μ M for *C. krusei*. Error bars show the standard error of the mean of 3 different experiments.